Supporting Information

Atomically dispersed Ru in Pt₃Sn intermetallic alloy as efficient methanol oxidation electrocatalysts

Tianyi Yang,[a] Fengjuan Qin,[a] Shuping Zhang,[a] Hongpan Rong,*[a] Wenxing Chen,*[a] Jiatao Zhang*[a]

Beijing Key Laboratory of Construction Tailorable Advanced Functional Materials and Green Applications, School of Materials Science and Engineering, Beijing Institute of Technology, Beijing 100081, China

Chemicals and Methods

1. Chemicals

Platinum(II) acetylacetonate (Pt(acac)$_2$, 97%), ruthenium(III) acetylacetonate (Ru(acac)$_3$, 97%), tin(II) chloride (SnCl$_2$, ≥ 99%), poly(vinylpyrrolidone)(PVP) and *N,N*-dimethylformamide (DMF), commercial Pt/C catalyst (20 wt% loading of Pt on carbon black) and Nafion (5%) were purchased from Alfa Aesar. Commercial PtRu/C catalyst (20 wt% loading of Pt and 10 wt% loading of Ru on carbon black) was purchased from Johnson Matthey. All the chemicals were used as received without further purification. The deionized water used in all experiments was prepared by passing through an ultrapure purification system (Aqua Solutions).

2. Synthesis of Pt$_3$Sn and Ru-Pt$_3$Sn Nanoconcaves (NCs)

In a typical synthesis of intermetallic Pt$_3$Sn NCs, platinum acetylacetonate (Pt(acac)$_2$, 9.8 mg), tin (II) chloride dehydrate (SnCl$_2$·2H$_2$O, 1.904 mg), poly(vinylpyrrolidone) (PVP, M. W. 30000, 80 mg) and *N, N*-dimethylformamide (DMF, 5 mL) were stirred for 20 min in an autoclave with volume of 10 mL. Then the autoclave was put into the oven at 180 °C. After 12 hours at 180 °C, the autoclave was cooled down till room temperature. The products were collected by centrifugation and washed three times with an ethanol/acetone mixture. Active carbon (Vulcan XC-72, 20 mg) was used to support the Pt$_3$Sn NCs. To synthesis Ru-Pt$_3$Sn NCs, ruthenium acetylacetonate (Ru(acac)$_3$, 0.64mg) was added into the autoclave with Pt$_3$Sn/C and DMF. The autoclave was put into the oven at 150 °C for 7 h. The products were collected by centrifugation and washed three times with an ethanol/acetone mixture.

Characterizations

The morphological characterization of these Ru-Pt$_3$Sn and Pt$_3$Sn NCs was conducted on a Hitachi JEM 2100F working at 200 kV. The X-ray diffraction (XRD) patterns were recorded with a Bruker D8 Discover diffractometer equipped with Cu Kα radiation (λ = 1.5418 Å). The X-ray photoelectron spectra (XPS) analysis was performed on Thermo escalab 250XI. The Thermo escalab 250XI instrument was equipped with an Al Kα source (hv= 1486.6 eV). The binding energy scale of all measurements was calibrated by referencing C 1s to 284.8 eV. High-angle annular dark-field (HAADF)

images were taken on a JEOL ARM-200 operated at 300 kV. Inductively coupled plasma-atomic emission spectroscopy (ICP-AES) was measured by a PROFILE SPEC instrument.

Electrochemical Measurements

The products were collected by centrifugation and washed five times with an ethanol mixture and were drying in vacuum oven. Three electrode system on an electrochemical workstation (CHI 660e) was used to carry out the electrochemical measurements. A glassy carbon rotating disk electrode (GCE, 5 mm diameter, 0.196 cm^2), Ag/AgCl (saturated KCl) electrode, Pt foil were used as working electrode, reference electrode, and counter electrode respectively. All electrochemical measurements were executed at room temperature. The solids product was used for the electrochemical measurement without further pre-treatment and were dispersed into mixed solvent (water: isopropanol: 5% Nafion = 4:1:0.025) at a concentration of 1 mg/mL. For electrochemical measurement, 13 μL suspension of this NCs/C catalyst was dropped on a GCE under infrared lamp. Methanol oxidation measurements were conducted in mixed solution of 0.1 M HClO$_4$ and 1 M methanol from -0.23 V to 0.96 V versus Ag/AgCl electrode at a scan rate of 50 mV s^{-1} from -0.23 V to 0.97 V (versus Ag/AgCl electrode). RHE = E + E$_{0 \text{ Ag/AgCl}}$ + 0.059pH is the conversion equation of potential between Reversible hydrogen electrode (RHE) and Ag/AgCl electrode. We used CV to represent that integrating the hydrogen adsorption charge electrochemical surface area (ECSA) measurements at room temperature in nitrogen saturated 0.1 M HClO$_4$ solution at a scan rate of 50 mV s^{-1}. Accelerated stability test was conduct on the same conditions. The chronoamperometry test was measured at 0.91 V for 3600 s in 1 M CH$_3$OH + 0.1 M HClO$_4$ solution. The ECSA was estimated by measuring the charge associated with H$_{upd}$ adsorption (Q$_H$). ECSA = Q$_H$/(q$_{H*}$m) and assuming 210 μC cm^{-2} for the adsorbed monolayer of hydrogen on Pt surface (q$_H$). The H$_{upd}$ adsorption charge (Q$_H$) could be determined by Q$_H$ = 0.5 × Q, where Q was the charge in the H$_{upd}$ adsorption/desorption area obtained after double-layer correction.

XAFS measurements

The Ru K-edge X-ray absorption data were collected at BL14W1 station in Shanghai

Synchrotron Radiation Facility (SSRF, operated at 3.5 GeV with a maximum current of 250 mA). At BL14W1, the radiation was monochromatized by a Si (311) double-crystal monochromator. The intensity of the incident X-ray was monitored by an Ar-filled ion chamber (I_0) in front of the sample. Solid samples were placed in an aluminum sample holder sealed with kapton tape. The data were collected as fluorescence excitation spectra with a Lytle detector. Energy was calibrated by the first peak maximum of the first derivative of a Ru foil (22117 eV), placed between two Ar-filled ionization chambers (I_1 and I_2) after the sample. The spectra of the references were recorded in transmission mode using an Ar-filled ionization chamber. All data were collected at room temperature.

XAFS Data Analysis

The acquired EXAFS data were processed according to the standard procedures using the Athena and Artemis implemented in the IFEFFIT software packages. The EXAFS spectra were obtained by subtracting the post-edge background from the overall absorption and then normalizing with respect to the edge-jump step. Subsequently, the $\chi(k)$ data of were Fourier transformed to real (R) space using a hanning windows (dk=1.0 Å^{-1}) to separate the EXAFS contributions from different coordination shells. To obtain the quantitative structural parameters around central atoms, least-squares curve parameter fitting was performed using the ARTEMIS module of IFEFFIT software packages.

The following EXAFS equation was used:

$$\chi(k) = \sum_j \frac{N_j S_0^2 F_j(k)}{k R_j^2} \exp[-2k^2\sigma_j^2]\exp\left[\frac{-2R_j}{\lambda(k)}\right]\sin[2kR_j+\varnothing_j(k)]$$

S_0^2 is the amplitude reduction factor, $F_j(k)$ is the effective curved-wave backscattering amplitude, N_j is the number of neighbors in the jth atomic shell, R_j is the distance between the X-ray absorbing central atom and the atoms in the jth atomic shell (backscatterer), λ is the mean free path in Å, $\phi_j(k)$ is the phase shift (including the phase shift for each shell and the total central atom phase shift), σ_j is the Debye-Waller parameter of the jth atomic shell (variation of distances around the average Rj). The

functions $F_j(k)$, λ and $\phi_j(k)$ were calculated with the ab initio code FEFF8.2. The coordination numbers of model samples were fixed as the nominal values. The obtained S_0^2 was fixed in the subsequent fitting. While the internal atomic distances R, Debye-Waller factor σ^2, and the edge-energy shift ΔE_0 were allowed to run freely.
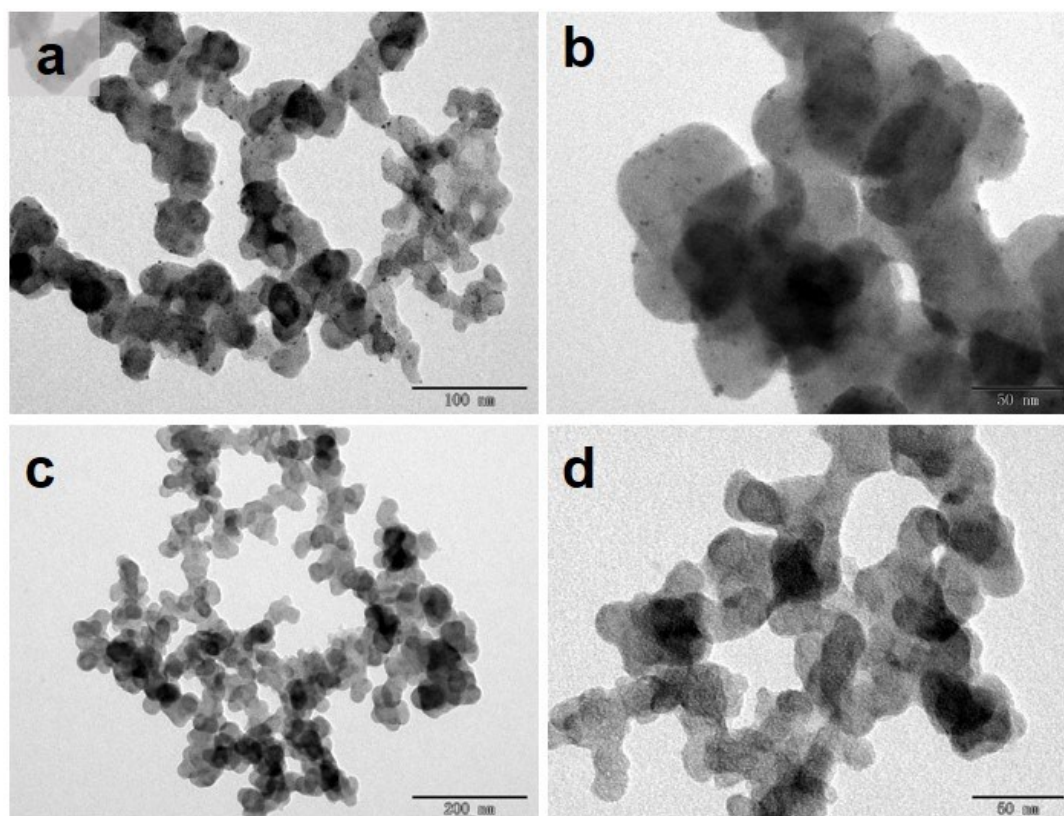
Figures and tables

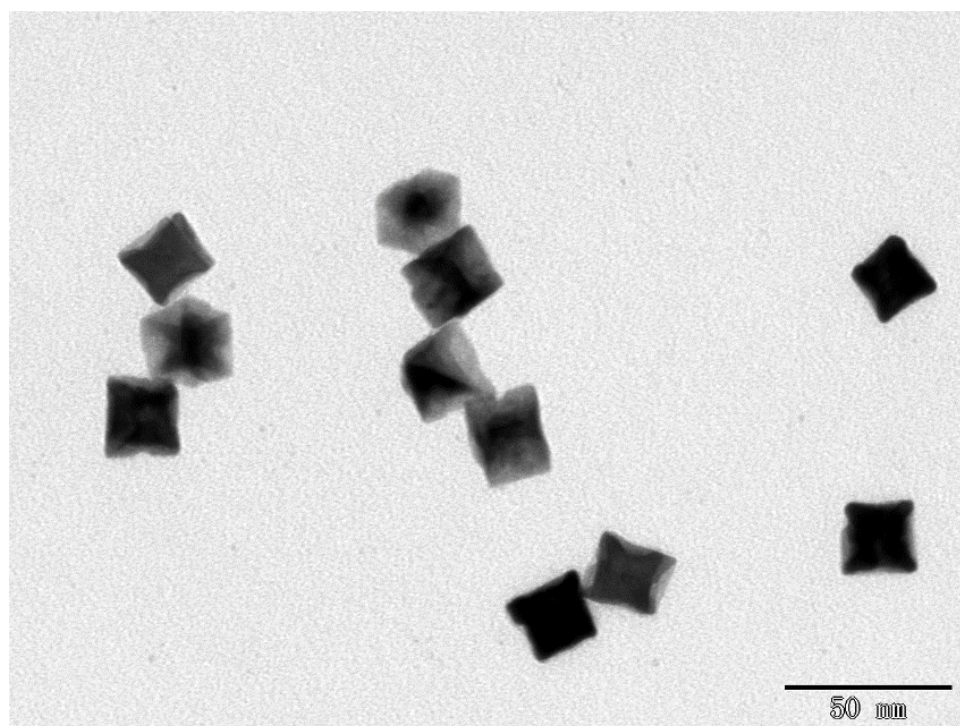Figure S1. TEM images of the Ru NPs/C prepared at (a, b) 170 °C and (c, d) 150 °C.

Figure S2. TEM image of the as-prepared Pt_3Sn NCs.
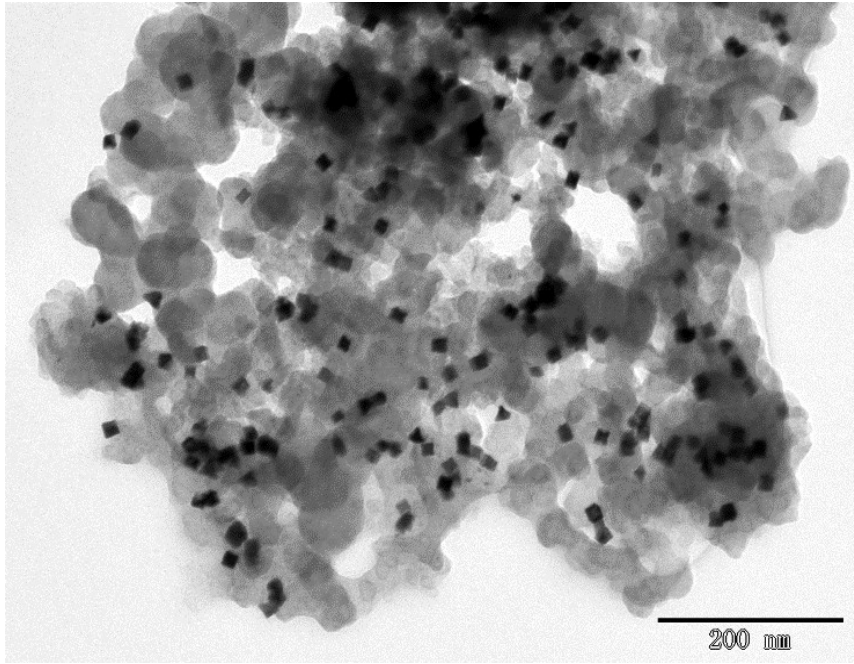
Figure S3. TEM image of the as-prepared Pt$_3$Sn NCs/C.
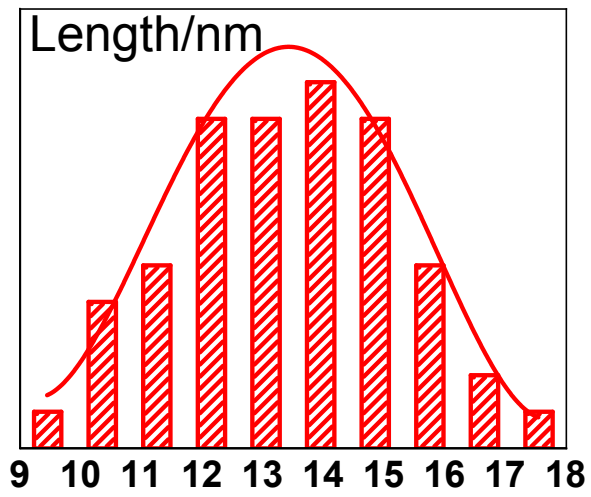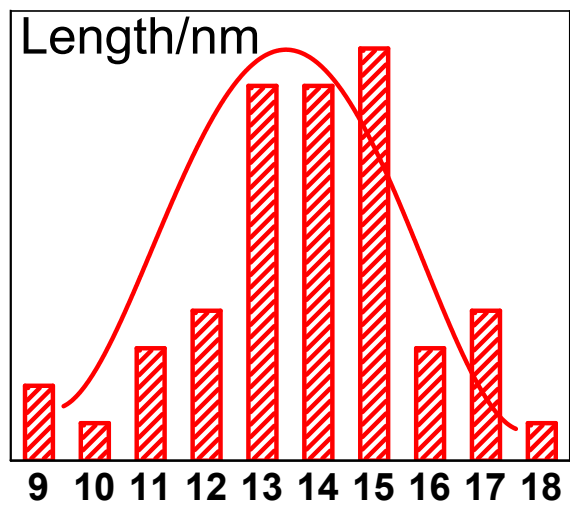
Figure S4. The histogram of length of the Ru-Pt$_3$Sn NCs.
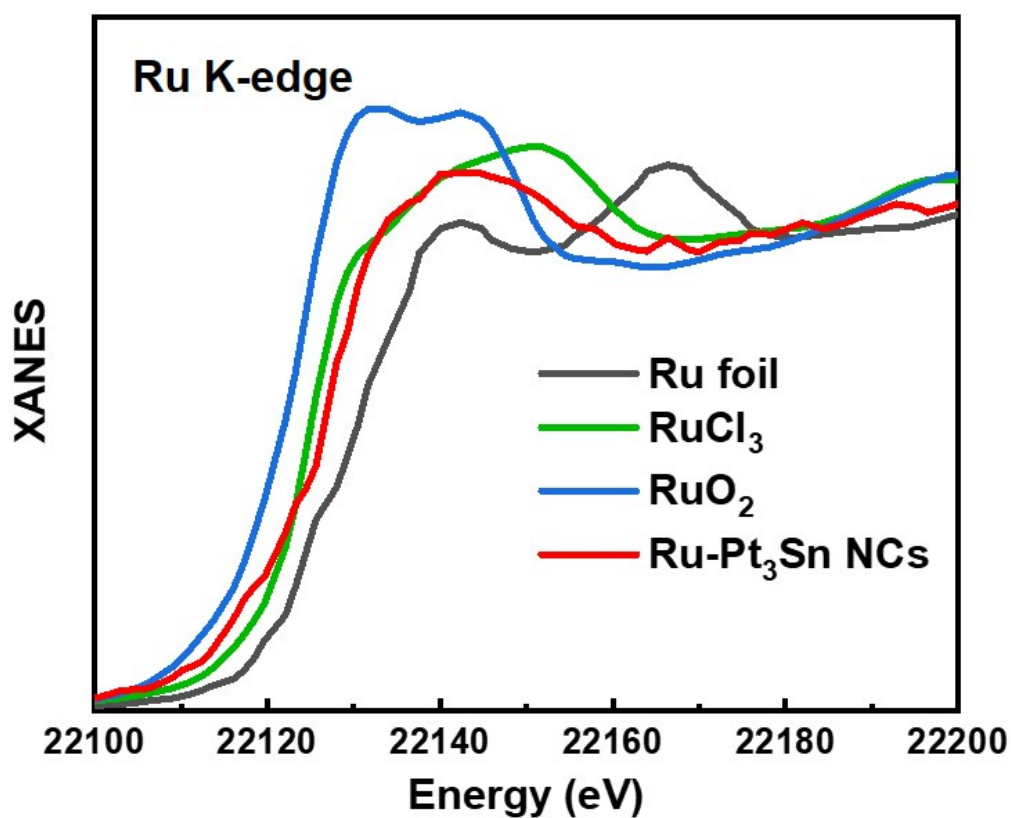

Figure S5. The histogram of length of the Pt$_3$Sn NCs.

Figure S6. The XANES curves of Ru K-edge for Ru-Pt$_3$Sn. Herein, Ru foil, RuCl$_3$ and RuO$_2$ are used as standard references.
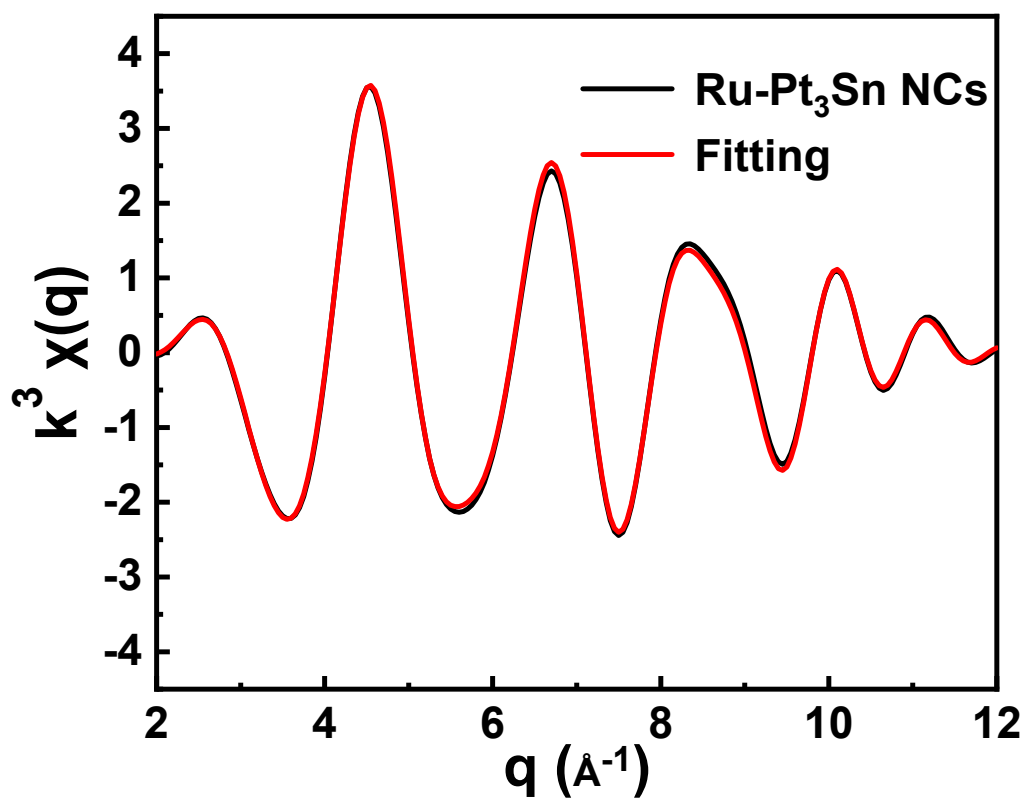

Figure S7. The q space EXAFS fitting curve of Ru-Pt$_3$Sn NCs at Ru K-edge.
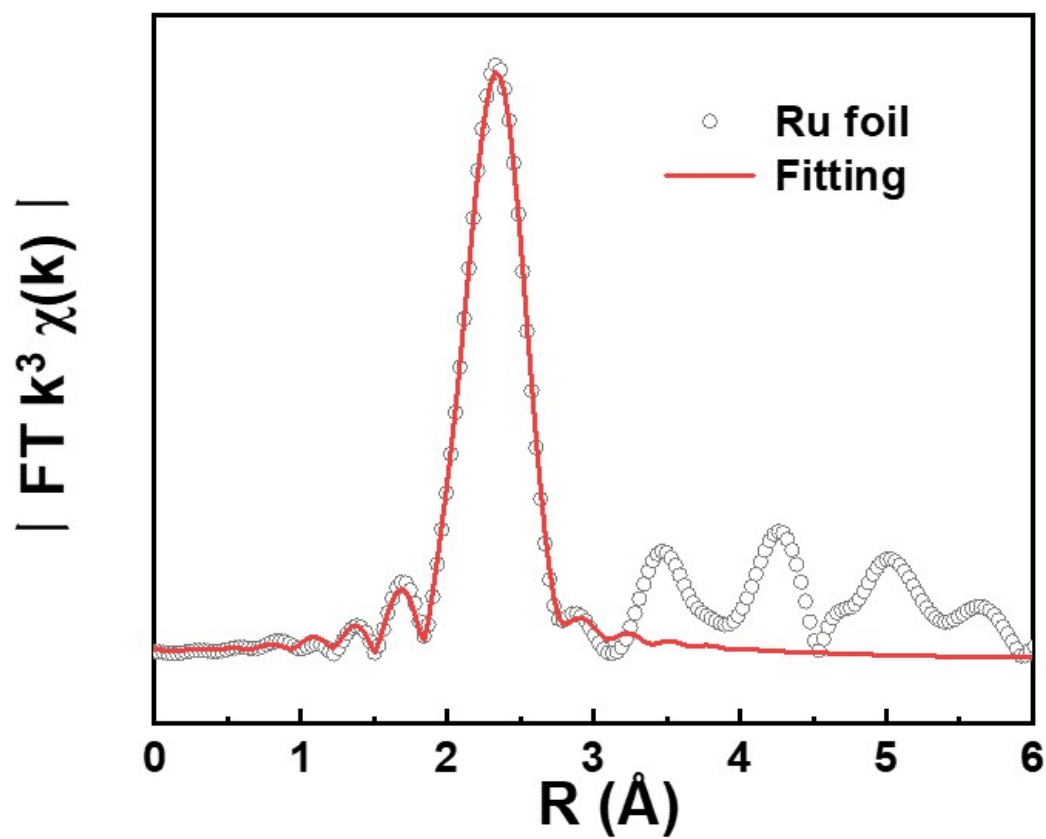
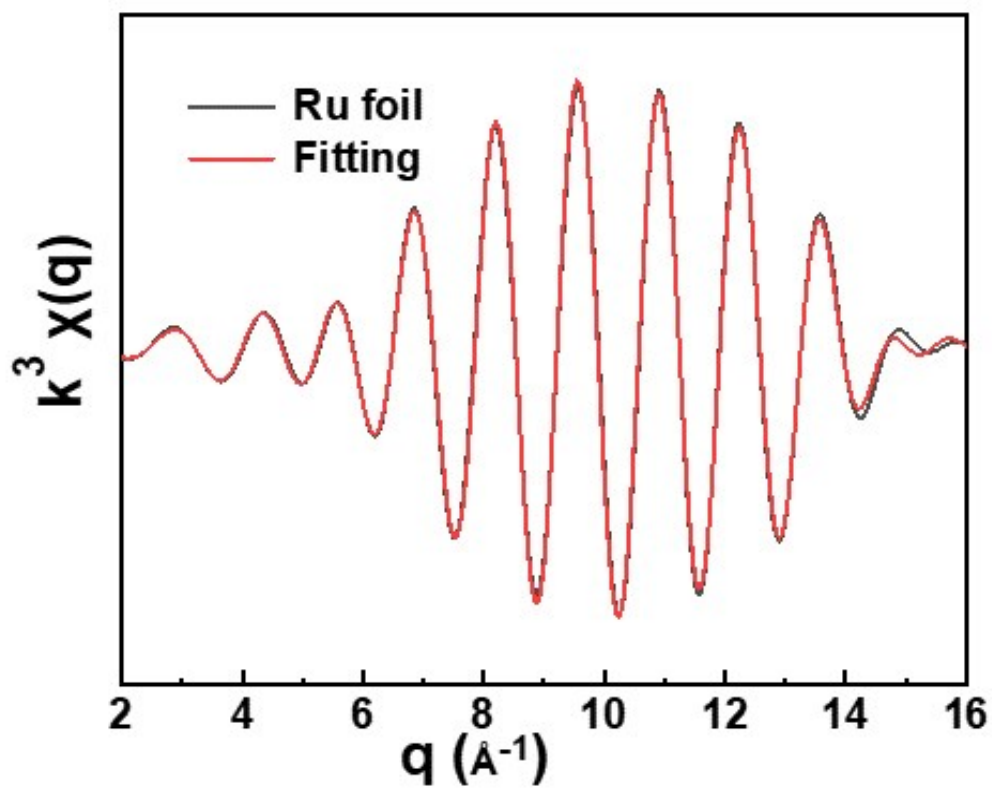Figure S8. FT-EXAFS fitting curves of the Ru foil at Ru K-edge.

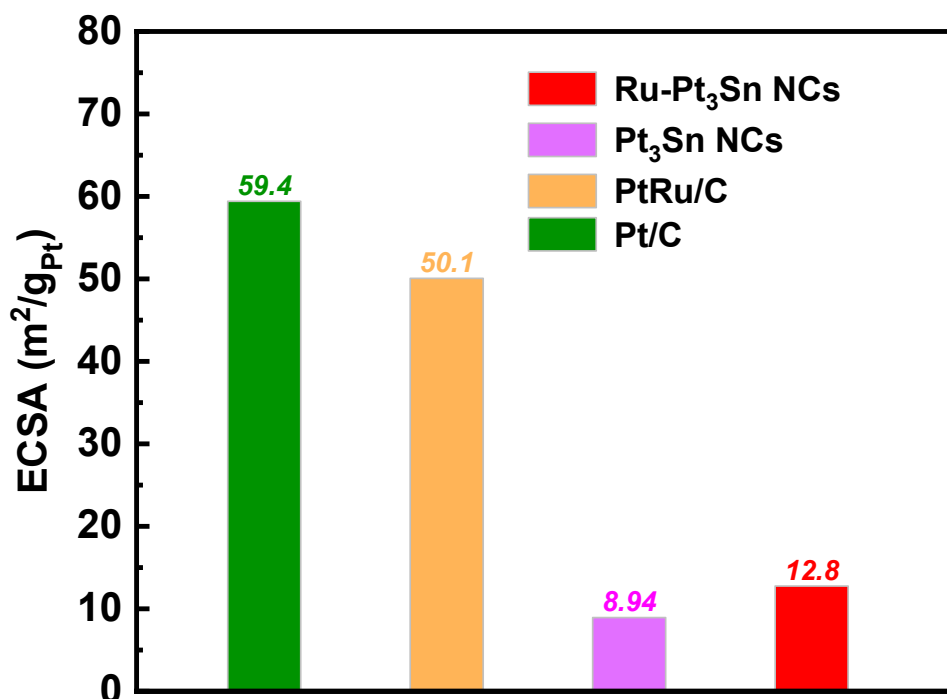Figure S9. The q space EXAFS fitting curve of Ru foil at Ru K-edge.

Figure S10. The ECSAs of Ru-Pt$_3$Sn NCs, Pt$_3$Sn NCs, commercial Pt/C and commercial PtRu/C recorded in 0.1 M HClO$_4$.
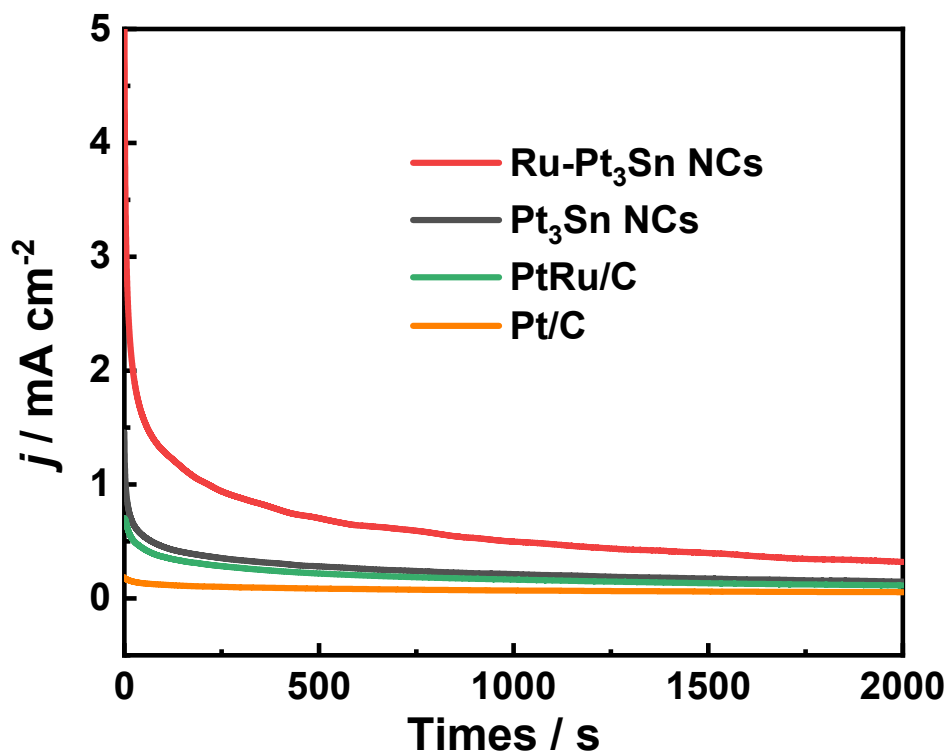

Figure S11. Chronoamperometry test for MOR at a potential of 0.91 V (vs. RHE) in 1 M CH$_3$OH + 0.1 M HClO$_4$ aqueous solution.
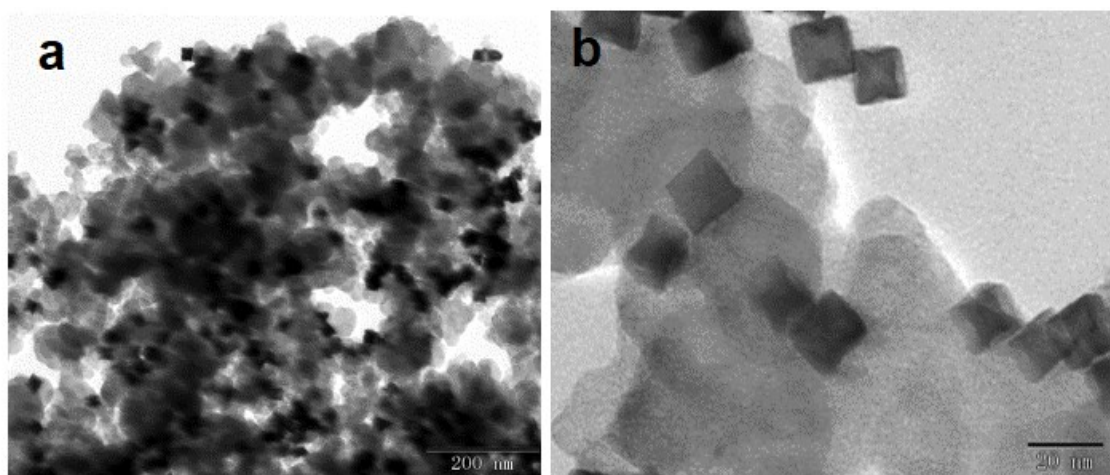
Figure S12. TEM images of the Ru-Pt$_3$Sn NCs after cycling stability tests.
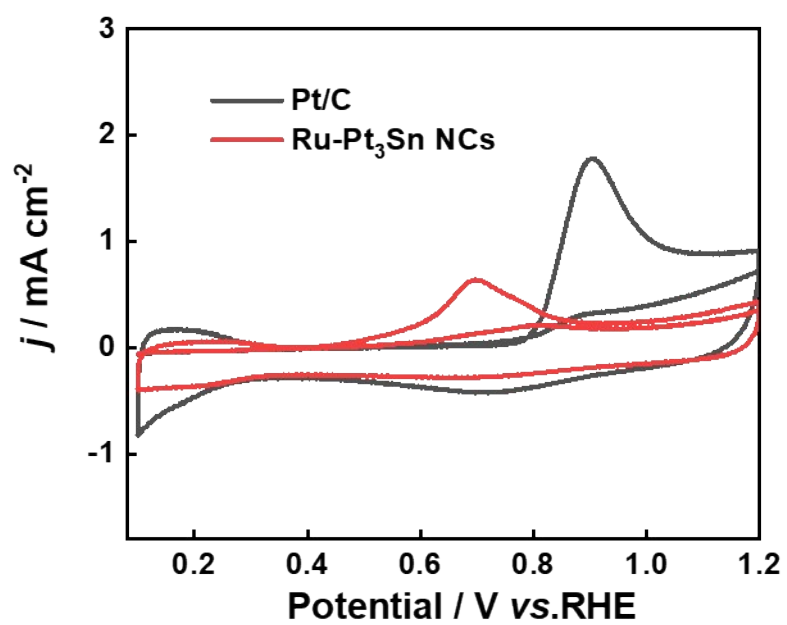

Figure S13. CO stripping voltammograms of Ru-Pt$_3$Sn NCs and commercial Pt/C catalysts in 0.1 M HClO$_4$. Pre-adsorption of CO on Pt was performed at 0.1 V vs. RHE.

Table S1 The edge length and Ru atomic ratio of the Ru-Pt$_3$Sn NCs.

	Pt$_3$Sn	Ru-Pt$_3$Sn NCs
Length (nm)	14.1±1.8	14.5±1.1
Ru Atomic ratio (%) by ICP	/	0.28

Table S2 Structural parameters extracted from the Ru K-edge EXAFS fitting. (S_0^2=0.81).

Sample	Scattering pair	CN	R (Å)	σ^2 (10^{-3} Å^2)	$\triangle E_0$(eV)	R factor
Ru-Pt$_3$Sn NCs	Ru-O	3.5	2.01	5.6	0.5	0.005
	Ru-Pt/Sn	2.3	2.65	6.7	0.5	
Ru foil	Ru- Ru$_1$	6*	2.65	3.3	0.5	0.006
	Ru- Ru$_2$	6*	2.72	3.5	0.5	

For the EXAFS fitting in Tables S2, S_0^2 is the amplitude reduction factor; CN is the coordination number; R is interatomic distance (the bond length between Ru central atoms and surrounding coordination atoms); σ^2 is Debye-Waller factor (a measure of thermal and static disorder in absorber-scatterer distances); ΔE_0 is edge-energy shift (the difference between the zero kinetic energy value of the sample and that of the theoretical model). R factor is used to value the goodness of the fitting.

* This value was fixed during EXAFS fitting, based on the known structure of Ru foil.

Error bounds that characterize the structural parameters obtained by EXAFS spectroscopy were estimated as N ± 20%; R ± 1%; σ^2 ± 20%; ΔE_0 ± 20%.

Table S3 The electrochemical properties of catalysts reported compared with our Ru-Pt$_3$Sn NCs catalyst.

Catalysts	SA/mA cm^{-2}	MA/mA ug^{-1}$_{Pt}$	Electrolytes	Reference
AL-Pt/Pt$_3$Ga	7.2	1.1	0.5 M H$_2$SO$_4$ + 1 M CH$_3$OH	1
Sub-4 nm PtZn/MWNT	1.2	0.6	0.5 M H$_2$SO$_4$ + 2 M CH$_3$OH	2
PtNiM/C (M = Rh, Os, and Ir)	2.8	1.8	0.1 M HClO$_4$ + 0.5 M CH$_3$OH	3
Trimetallic PtSnRh	/	0.6	0.1 M NaOH + 0.1 M CH$_3$OH	4
Durable Pt$_{72}$Ru$_{28}$	11.5	1.8	0.1 M HClO$_4$ + 0.5 M CH$_3$OH	5
Pt-Ru Nanocrystals	1.2	0.86	0.1 M HClO$_4$ + 0.5 M CH$_3$OH	6
Pt-Co/C nano-branched	5.7	2.7	0.1 M HClO$_4$ + 0.5 M CH$_3$OH	7
PtRu Dilute Alloy	2.66	1.14	0.1 M HClO$_4$ + 0.5 M CH$_3$OH	8
Ru-Pt$_3$Sn NCs	4.6	0.74	0.1 M HClO$_4$ + 1 M CH$_3$OH	This work

Reference

1. Q. Feng, S. Zhao, D. He, S. Tian, L. Gu, X. Wen, C. Chen, Q. Peng, D. Wang and Y. Li, *J. Am. Chem. Soc.,* 2018, **140**, 2773-2776.

2. Z. Qi, C. Xiao, C. Liu, T. W. Goh, L. Zhou, R. Maligal-Ganesh, Y. Pei, X. Li, L. A. Curtiss and W. Huang, *J. Am. Chem. Soc.*, 2017, **139**, 4762-4768.

3. W. Zhang, Y. Yang, B. Huang, F. Lv, K. Wang, N. Li, M. Luo, Y. Chao, Y. Li, Y. Sun, Z. Xu, Y. Qin, W. Yang, J. Zhou, Y. Du, D. Su and S. Guo, *Adv. Mater.*, 2019, **31**, 1805833.

4. K. Jiang, L. Bu, P. Wang, S. Guo and X. Huang, *ACS Appl. Mater. Interfaces*, 2015, **7**, 15061-15067.

5. W. Y. Zhao, B. Ni, Q. Yuan, P. L. He, Y. Gong, L. Gu and X. Wang, *Adv. Energy Mater.*, 2017, **7**, 1601593.

6. L. Huang, X. Zhang, Q. Wang, Y. Han, Y. Fang and S. Dong, *J. Am. Chem. Soc.*, 2018, **140**, 1142-1147.

7. W. Lei, M. Li, L. He, X. Meng, Z. Mu, Y. Yu, F. M. Ross and W. Yang, *Nano Res.*, 2020, **13**, 638-645.

8. S. Zhang, H. Rong, T. Yang, B. Bai and J. Zhang, *Chem. Eur. J.*, 2019, 4025-4031.